Asymmetry of localised states in a single quantum ring: polarization dependence of excitons and biexcitons

H. D. Kim[1], K. Kyhm[2,3],* R. A. Taylor[1],† G. Nogues[2], K. C. Je[4], E. H. Lee[5], and J. D. Song[5]
[1] *Clarendon Laboratory, Department of Physics, University of Oxford, Oxford, OX1 3PU, U.K*
[2] *Department of NANOscience, Institut Néel, CNRS, rue des Martyrs 38054, Grenoble, France*
[3] *Department of Physics Education, RCDAMP, Pusan Nat'l University, Busan 609-735, South Korea*
[4] *College of Liberal Arts and Sciences, Anyang University, Gyeonggi-do 430-714, South Korea and*
[5] *Nano-Photonics Research Center, KIST, Seoul, 136-791, South Korea*
(Dated: January 28, 2013)

We performed spectroscopic studies of a single GaAs quantum ring with an anisotropy in the rim height. The presence of an asymmetric localised state was suggested by the adiabatic potential. The asymmetry was investigated in terms of the polarization dependence of excitons and biexcitons, where a large energy difference (~ 0.8 meV) in the exciton emission energy for perpendicular polarizations was observed and the oscillator strengths were also compared using the photoluminescence decay rate. For perpendicular polarizations the biexciton exhibits twice the energy difference seen for the exciton, a fact that may be attributed to a possible change in the selection rules for the lowered symmetry.

Currently, quantum ring (QR) structures are of great interest for the optical Aharonov-Bohm (AB) effect [1–5]. While the rotating charge in the shell of a type-II quantum dot (QD) determines the AB oscillation period, the orbital radius difference of the electrons and holes is the crucial parameter in a QR, for which the coupling to the magnetic flux is of opposite sign. Nevertheless, the individual behaviour of each of the particles is not clear in a QR; either the radius is larger or one of them is localised as in the case of a type-II QD.

Recent measurements have shown that the morphology of a QR is anisotropic, where the rim height is not constant around the azimuthal angle. In the case of this so-called volcano-like structure [5], the azimuthal quantum number is no longer valid, and the wavefunction in the anisotropic QR can be either localised or delocalised through tunnelling [6]. Nevertheless, a persistent current can be observed in a QR as evidence of AB-oscillation, when an external magnetic field is large enough to overcome the anisotropy-induced potential barrier or asymmetric exchange interaction [4]. Asymmetry and anisotropy seem to have been overlooked in the spectroscopy of QRs [1–3, 7–9]. In this work, the presence of a localised state in a single GaAs/$Al_{0.3}Ga_{0.7}As$ QR arises from the volcano-like QR structure, which corresponds to an excited state of the vertical confinement. Also, the asymmetry of the localised state has been investigated in terms of the polarization dependence of excitons and biexcitons.

GaAs rings [7] were grown on an n-doped GaAs (001) substrate using a molecular beam epitaxy system with an ion getter pump. After thermal cleaning of the substrate under arsenic ambient at 600°C, a 100 nm-thick GaAs buffer layer and a 50 nm-thick $Al_{0.3}Ga_{0.7}As$ layer were grown successively at 580°C. The substrate temperature was decreased to 310°C, and Ga metal equivalent to 2 monolayers of GaAs was introduced to the substrate at the main chamber pressure of $\sim 3\times10^{-10}$ Torr. When the substrate temperature reached 200°C, arsenic tetramers were introduced to form GaAs rings. Finally, the rings were capped with 60 nm-thick $Al_{0.3}Ga_{0.7}As$ and 3 nm-thick GaAs for optical measurements. The photoluminescence (PL) of a single QR was collected at 4 K using a confocal arrangement, where frequency-doubled (400 nm) Ti:sapphire laser pulses (120 fs pulse duration at a 80-MHz repetition rate) were focused on the QR sample (~ 6 QRs/μm^2) with a spot-size of 0.8 μm^2. A time-correlated single photon counting system was used to obtain the time-resolved PL (TRPL).

As shown in Fig.1(a), the volcano-like ring structure was modelled in cylindrical coordinates ($z = z(r,\phi)$) based on atomic force microscope (AFM) images of uncapped GaAs QRs (Fig.1(b)), where both anisotropy and asymmetry are present [7, 10]. The rim height is maximum at the azimuthal angles of 0° and 180° along the $[1\bar{1}0]$ direction, and a minimum at the perpendicular angles of 90° and 270° along the [110] direction, respectively. The in-plane shape is elliptical with the long axis along $[1\bar{1}0]$, and the height in the middle of the QR is ~ 3 nm. Since the vertical height ($7 \sim 12$ nm) is smaller than the ring size (~ 50 nm), the fast vertical wavefunction can be separated by the adiabatic approximation [5], where the potential of electron and hole depends on the volcano-like ring structure respectively as $V_{e,h}(z,r,\phi) \simeq V_{e,h}(z(r,\phi))$. Consequently, the adiabatic potential $\varepsilon^k_{e,h}(r,\phi)$ can be obtained for electron and hole separately by solving the vertical part of the Schrödinger equation, where the vertical confinement is represented by the vertical quantum number k. In the case of an ideal isotropic ring, $\varepsilon^k_{e,h}(r)$ can be simplified by using a parabolic function ($\sim (r-r_0)^2$), where the maximum ring height is positioned at r_0 [11]. Although the fine structure of the PL spectrum in a QR has often been attributed to quantized

*Electronic address: kskyhm@pusan.ac.kr
†Electronic address: r.taylor1@physics.ox.ac.uk

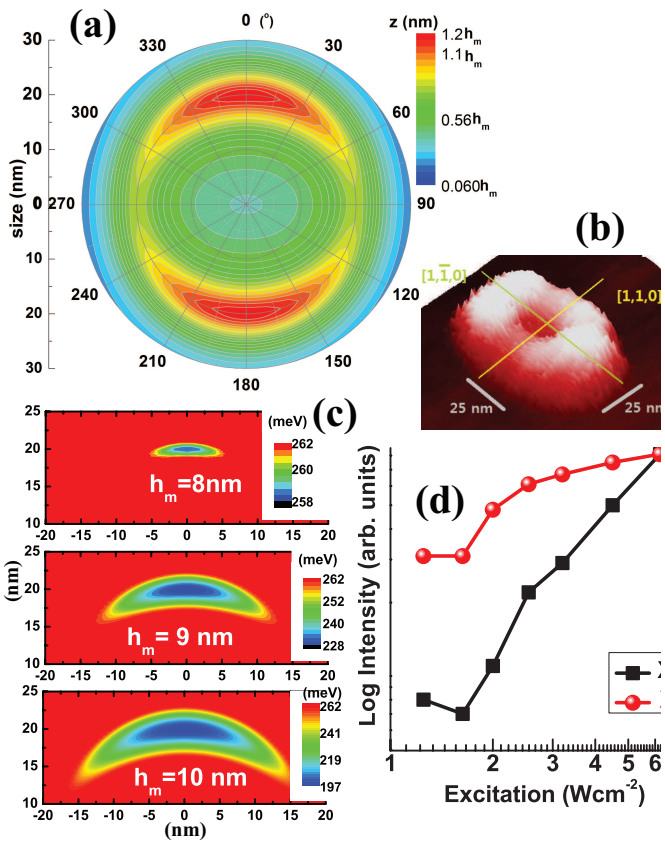

FIG. 1: (a) Volcano-like ring model for the rim height based on the AFM morphology (b), where the localised adiabatic potentials of the electron for a vertical quantum number of $k = 3$ are shown for three rim height parameters ($h_{\rm m} = 8, 9, 10\,{\rm nm}$) (c). (d) PL intensity corresponding to the $k = 3$ states from the XX is compared with that from the X with increasing the excitation power.

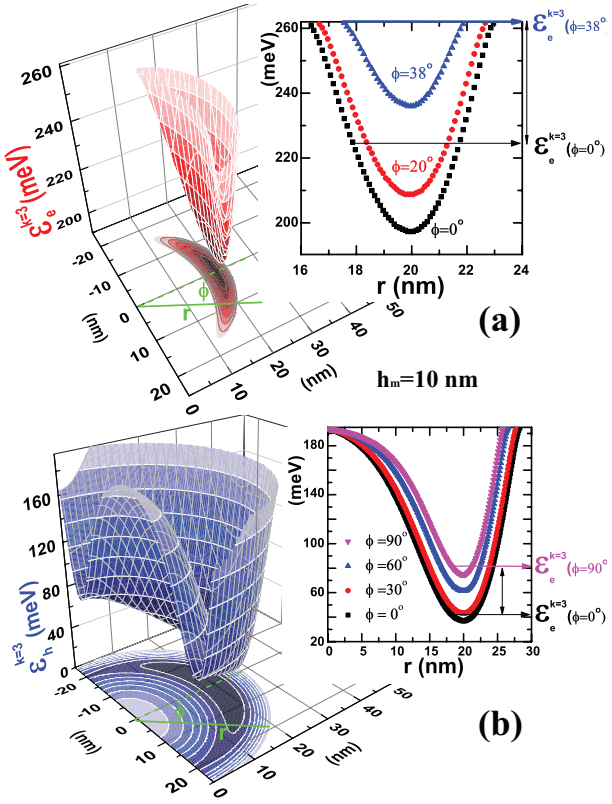

FIG. 2: Adiabatic potentials ($\varepsilon_{\rm e,h}^{k=3}$) of the electron (a) and the hole (b) for a vertical quantum number of $k = 3$ are shown, where the insets show the energy range of the radially confined levels for the azimuthal angle for the electron and the hole, respectively.

rotational motion along the rim [7], the cylindrical symmetry of a QR can easily break down, which is similar to the case of an elliptical QD. Also, the anisotropy in the rim height requires an azimuthal angle-dependence of the vertical confinement. Both the asymmetry of the in-plane ellipticity and the height anisotropy have been mostly overlooked in previous spectroscopy. These effects can be paramaterized in terms of $\varepsilon_{\rm e,h}^{k}(r,\phi)$, which is similar to an inversion of the asymmetric and anisotropic structure morphology.

Provided that the potential hill in $\varepsilon_{\rm e,h}^{k}(r,\phi)$ is found near the azimuthal angles 90° and 270°, the wavefunction delocalisation of the ground state depends on the tunneling efficiency, which determines either localised [6] or extended states. However, it should be remembered that the number of confinement states can be a measure of the confinement size, i.e., the higher rim (z) contains more vertical confinement states than the lower rim. In other words, excited confinement states are allowed only at the limited azimuthal angles of the high rim region as the k quantum number increases [5]. We found that vertical confinement states can be defined at all of the azimuthal angles up to $k = 2$. Therefore, the vertical excited state of $k = 3$ is a criterion of the localisation. As shown in Fig.1(c), the electron adiabatic potentials for $k = 3$ ($\varepsilon_{\rm e}^{k=3}(r,\phi)$) are localised at limited azimuthal angles for three different QR heights ($h_{\rm m} = 8, 9, 10\,{\rm nm}$), where the rim height is characterized by a parameter $h_{\rm m}$[10]. As the QR height is decreased, the localized potential area becomes reduced.

The adiabatic potentials of the electron ($\varepsilon_{\rm e}^{k=3}$) and hole ($\varepsilon_{\rm h}^{k=3}$) are compared for $h_{\rm m} = 10\,{\rm nm}$ in Fig.2 [12]. Also, the radially confined energy of the adiabatic potential for $\phi = 0°$ and $\phi = 90°$ are estimated with the parabolic approximation for the electron and the hole (insets in Fig.2), respectively. Whilst the holes are confined for all azimuthal angles (Fig.2-(b)), the electron is confined to the limited azimuthal angles ($-38° \sim 38°$) (Fig.2-(a)) due to the shallow potential well when compared to the barrier energy in the conduction band (262 meV).

Therefore, the ground eigen-energy of the electron and the hole should be located in the range of the radially confined levels for allowed azimuthal angles ($\varepsilon_{\mathrm{e,h}}^{k=3}(\phi)$). For example, suppose the ground state of the electron is located near 240 meV, then the confined wavefunction becomes localised in a crescent-like structure. However, the tunnelling wavefunction is extended up to ~ 4.5 nm in the barrier. On the other hand, the hole wavefunction also becomes localised when the hole ground state is assumed to be $\sim$ 60 meV, but the tunnelling length is small (~ 0.7 nm) as the barrier energy in the valence band (195 meV) is still large. Consequently, the localised area of the electron would be larger due to the large tunnelling, and PL quenching becomes significant with increasing temperature. We found the PL intensity is nearly quenched beyond ~ 45 K.

The exact ground state energy of the electron-hole (e-h) pair can be refined by adding the Coulomb interaction to the independent e-h pair, i.e., the total energy is determined by the ground state energy sum of each adiabatic potential and the Coulomb energy. In the case of strong confinement, the effective Coulomb interaction is known to be enhanced by a factor of 1.786. However, both the vertical and the lateral confinement energy are far larger than the Coulomb interaction (~ 4.2 meV for bulk GaAs). Thus, the energy levels are dominated by the confinement effect, and this rough model predicts the energy range of the e-h pair at the $k = 3$ state ($1.814 \sim 1.864$ eV). As shown in Fig.3, the PL spectrum was measured near the barrier ($Al_{0.3}Ga_{0.7}As$) energy. It exhibits a strong polarization dependence for the exciton (X) and biexciton (XX) states at 1.6 kWcm^{-2}, where the nature of the XX emission appearing 5 meV below that of the X was characterised by a quadratic rise in its PL intensity (Fig.1(d)) and the fast decay of the TR-PL (Fig.4(b)) relative to the X. The X and XX emission spectra were both measured simultaneously at a series of analyzer angles. We also observed the PL spectrum in the predicted $k = 3$ range (1.813 eV, 1.821 eV, 1.832 eV, and 1.842 eV) at different QRs; they all show the similar polarization dependence.

The wavefunction of the electron and the hole can be imagined roughly as an inversion structure of the adiabatic potential in Fig.2. Since both $\varepsilon_{\mathrm{e}}^{k=3}$ and $\varepsilon_{\mathrm{h}}^{k=3}$ are anisotropic, the e-h pair is likely to be localised in either of the two crescent structures instead of delocalization around the whole rim. The localised e-h pair can be verified in terms of the large energy splitting for perpendicular polarizations. Since the localised states are of a crescent shape, the fine structure states resulting from various different confinement dimensions may depend on the analyzer angle. Additionally, during sample growth, identical crescents are unlikely to form in an anisotropic QR and the resonance at the $k = 3$ state between the two crescents is vulnerable to small size differences. In this case, localisation of the e-h pair is favored at the larger crescent-like structure.

Whilst the two orthogonally polarized states of $|X\rangle$ and $|Y\rangle$ in an elliptical QD can be spectrally isolated by a linear polarizer [13–15], the fine structure states at different angles in the asymmetric $\varepsilon^{k=3}(r,\phi)$ can overlap in the PL spectrum of X. Therefore, the analyzer angle dependence of the PL intensity is mapped at different energies in polar coordinates as shown in Fig.3(b), where the maximum intensity of each PL spectrum is normalized to make a comparison possible. For example, the maximum PL intensity of X at 1.8208 eV measured at 0° is gradually reduced until the analyzer angle rotates to 90°, but increases again up to 180°. Consequently, this sinusoidal behavior gives rise to a dumbbell-like trace. All of the dumbbell-like traces obtained at different energies are similar, but rotated in a regular manner. The relative angular delay (θ) between the traces varies with emission energy. The trace at 1.8200 eV is 90°-rotated with respect to that at 1.8208 eV, and an energy difference (Δ) of 0.8 meV is obtained. This value is remarkably large in comparison to the asymmetric splitting ($\Delta_{XY} \sim 0.1$ meV) of an elliptical quantum dot.

In the case of an elliptical quantum dot, an asymmet-

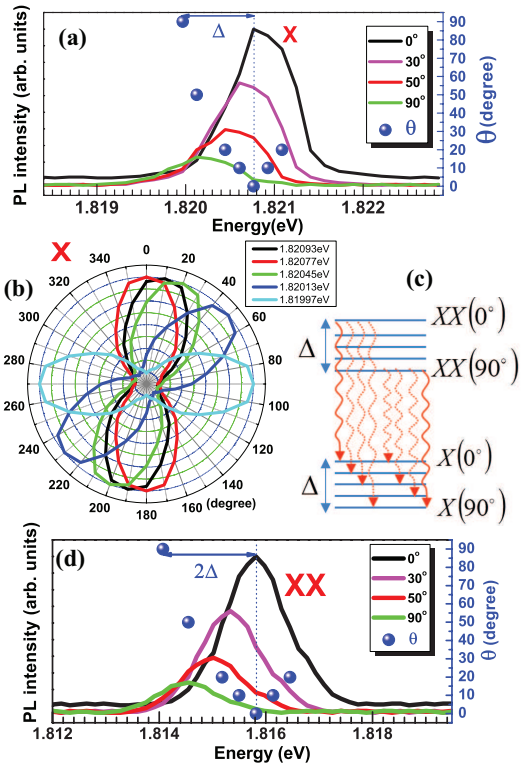

FIG. 3: PL spectrum of the X (a) and XX (d) at various analyzer angles in a single QR. (b) Normalized PL intensity as a function of analyzer angle is mapped in polar coordinates at various energies, whereby the relative angular delay (θ) of each dumbbell-like trace can be obtained for the X and XX. (c) Schematic diagram of a multitude of transitions between the fine structure states of XX and X.

ric electron-hole exchange interaction leads to a splitting (Δ_{XY}) of the double exciton state ($|\pm 1\rangle$) into two singlet states ($|X,Y\rangle = (|+1\rangle \pm |-1\rangle)/\sqrt{2}$), where two linearly and orthogonally polarized dipoles ($|X\rangle$ and $|Y\rangle$) are defined along the principal axes of an elliptical QD [13–15]. This also gives rise to the same splitting of the biexciton emission (Δ_{XY}), which involves the transition from biexciton to two singlet exciton states ($|X,Y\rangle$), respectively. However, the energy difference for the perpendicular polarization in the XX spectrum (Fig.3(d)) is nearly twice (~ 1.75 meV) that of X, where the angular delay of 90° is measured by the dumbbell-like trace of XX. We have also confirmed this phenomenon in QRs of different sizes.

When considering XX in this structure, two kinds of generation are possible; either two Xs in the same localised crescent structure or separate Xs located in two identical crescent structures are bound, respectively. Although the binding energy of the latter case was known to be sub-meV[6], the generation can be inhibited by the small size difference between the two crescent structures. For large GaAs QDs (30 $\sim$ 40 nm in radius), the XX binding energy is known to be a few meV [17, 18]. Therefore, the large binding energy (~ 5 meV) in this result is likely to arise from a localised XX, which consists of two Xs localised at the same crescent structure. The large asymmetric splitting ($\Delta_{XY} \sim 1.75$ meV) of the XX also supports a localised XX. When the symmetry is lowered, it is known that the selection rules change significantly [16, 19]. This can give rise to an increase in the number of dipole-allowed transitions, i.e., a multitude of transitions between the two-exciton and one-exciton states, resulting in a broad PL spectrum for the XX. It is also noticeable that the XX PL spectrum in Fig.3(d) is rather broad. Consequently, as shown schematically in Fig.3(c), a multitude of transitions between the fine structure states of XX and X, which are denoted by the relative angular delay (θ), may result in twice the splitting when compared to the X for perpendicular polarizations because of the change in the ideal selection rules.

Although the wavefunction distribution of the fine structure states is not clear, the oscillator strength difference of these states can be observed in terms of the size dependence of the PL decay rate, where the PL spectra for different confinement sizes are isolated by the analyzer angle. As shown in Fig.4, TRPL of X and XX was measured at various analyzer angles (θ), where the PL decay rates were obtained by a linear fit to the monotonic decay section on a log scale (shown in the inset). We found that the PL decay rates of both X and XX increase for increasing analyzer angle up to 90°. Interestingly, XX shows a novel feature in the size dependent oscillator strength.

Whilst the radiative recombination of the e-h pair is characterized by a single exponential decay after $\sim$ 400 ps, a plateau range is observed up to $\sim$ 300 ps in Fig.4(a). This may be associated with extended states of the electron. Initially, e-h recombination occurs at the wavefunction overlap range between the localised electron and hole. However, extended states keep feeding electrons to localised states. State saturation in the plateau suggests the presence of a feeding source for intra-relaxation of localised electrons ($k = 3$) to lower states ($k = 2$ or $k = 1$). Furthermore, it is noticeable that the decay time (532 ± 56 ps) of the X is longer than that seen in GaAs QDs (250 ± 50 ps) [13]. When compared to the recombination rate of a hole near localised electrons, the recombination rate of a hole far from such localised electrons can be reduced. This effect possibly results in the reduction of the total decay rate in the $k = 3$ localised structure.

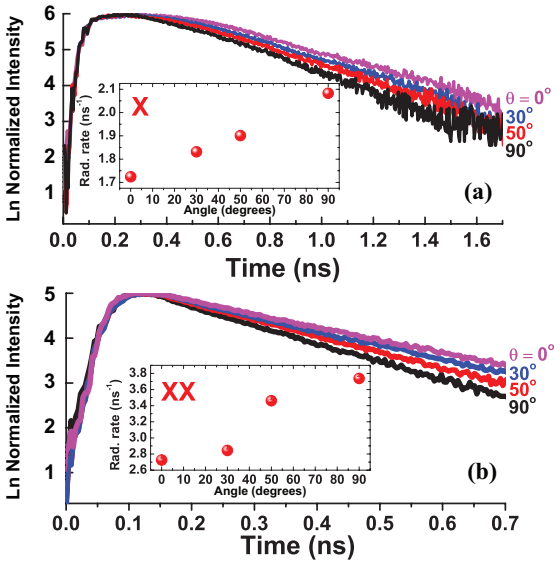

FIG. 4: TRPL of the of the localised state of X (a) and XX (b) in a single QR measured at 1.6 kWcm^{-2} for various analyzer angles, where each PL rate shown in the inset.

In conclusion, the presence of an asymmetric localised state in a single GaAs/$Al_{0.3}Ga_{0.7}As$ QR was observed by its polarization dependence in the PL spectrum, which is in agreement with the adiabatic potential arising from a volcano-like anisotropic morphology. The fine structure states of the crescent-like adiabatic potential were resolved by changing the analyzer angle, whereby a large energy difference in the exciton (~ 0.8 meV) and biexciton (~ 1.75 meV) splitting was observed for perpendicular polarizations, and oscillator strength differences were also compared in terms of the PL decay rate.

Acknowledgments

This work was supported by the National Research Foundation of Korea Grant funded by MEST (NRF-2011-013-C00025 and NRF-2010-008942) and GRL program, and the KIST institutional program. Authors are also grateful to the late Dr. Lee for organizing the international collaboration.

[1] M. Bayer, M. Korkusinski, P. Hawrylak, T. Gutbrod, M. Michel, and A. Forchel, Phys. Rev. Lett. **90**, 186801 (2003).

[2] A. O. Govorov, S. E. Ulloa, K. Karrai, R. J. Warburton, Phys. Rev. B **66**, 081309(R) (2002).

[3] E. Ribeiro, A. O. Govorov, W. Carvalho, Jr., and G. Medeiros-Ribeiro, Phys. Rev. Lett. **92**, 126402 (2004).

[4] N. A. J. M. Kleemans, I. M. A. Bominaar-Silkens, V. M. Fomin, V. N. Gladilin, D. Granados, A. G. Taboada, J. M. Garcia, P. Offermans, U. Zeitler, P. C. M. Christianen, J. C. Maan, J. T. Devreese, and P. M. Koenraad, Phys. Rev. Lett. **99**, 146808 (2007).

[5] V. M. Fomin, V. N. Gladilin, S. N. Klimin, and J. D. Devreese, N. A. J. M. Kleemans, and P. M. Koenraad, Phys. Rev. B **76**, 235320 (2007).

[6] T-C Lin, C-H Lin, H-S Ling, Y-J Fu, W-H Chang, S-D Lin, and C-P Lee, Phys. Rev. B **80**, 081304(R) (2009).

[7] T. Kuroda, T. Mano, S. Sanguinetti, K. Sakoda, G. Kido, and N. Koguchi, Phys. Rev. B **72**, 205301 (2005).

[8] R. J. Warburton, C. Schulhauser, D. Haft, C. Schaflein, K. Karrai, J. M. Garcia, W. Schoenfeld, and P. M. Petroff Phys. Rev. B **65**, 113303 (2002).

[9] B. Alen, J. Martinez-Pastor, D. Granados, and J.M. Garcia, Phys.Rev.B **72**, 155331 (2005).

[10] $R = 20\,\mathrm{nm}$, $h_0 = 4\,\mathrm{nm}$, $h_\infty = 0.4\,\mathrm{nm}$, $\gamma_0 = 5.5\,\mathrm{nm}$, $\gamma_\infty = 5.5\,\mathrm{nm}$, $\xi_\mathrm{h} = 0.2$, $\xi_\gamma = 0$, and $\xi_\mathrm{R} = 0$, where all parameters are defined in [5], and the effective mass and band-offset of electron and hole of GaAs and AlGaAs are given in [7].

[11] J. Song and S.E. Ulloa, Phys. Rev. B **63**, 125302 (2001).

[12] While $k = 3$ is the largest vertical quantum number for electron, higher $k(> 3)$ are possible in the valence band. However, the corresponding energy is beyond the observed PL spectrum, and the accuracy is limited for ignorance of the spin-orbit coupling.

[13] I. Favero, G. Cassabois, C. Voisin, C. Delalande, Ph. Roussignol, R. Ferreira, C. Couteau, J. P. Poizat, and J. M. Gerard, Phys. Rev. B **71**, 233304 (2005).

[14] H. Htoon, S. A. Crooker, M. Furis, S. Jeong, Al. L. Efros, and V. I. Klimov, Phys. Rev. Lett.**102**, 017402 (2009).

[15] H. Htoon, M. Furis, S. A. Crooker, S. Jeong, and V. I. Klimov, Phys. Rev. B **77**, 035328 (2008).

[16] M. P. Nowak and B. Szafran, Phys. Rev. B **80**, 195319 (2009).

[17] M. Ikezawa, S. V. Nair, H-W. Ren, Y. Masumoto, and H. Ruda, Phys. Rev. B **73**, 125321 (2006).

[18] J-W. Luo and A. Zunger, Phys. Rev. B **84**, 235317 (2011).

[19] H. Giessen, U. Woggon, B. Fluegel, G. Mohs, Y. Z. Hu, S. W. Koch, and N. Peyghambarian, Opt. Lett. **21**, 1043 (1996).